

EPR Analysis and DFT Computations of a Series of Polynitroxides

M. Francesca Ottaviani,^{*†} Alberto Modelli,[‡] Olaf Zeika,[§] Steffen Jockusch,[§] Alberto Moscatelli,[§] and Nicholas J. Turro[§]

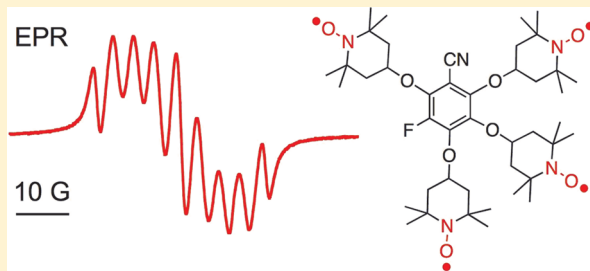
[†]Department of Earth, Life and Environment Sciences (DiSTeVA), University of Urbino, 61029 Urbino, Italy

[‡]Department of Chemistry “G. Ciamician”, University of Bologna, 40126 Bologna, Italy, and Centro Interdipartimentale di Ricerca in Scienze Ambientali (CIRSA), 48123 Ravenna, Italy

[§]Department of Chemistry, Columbia University, New York, New York 10027, United States

 Supporting Information

ABSTRACT: Polynitroxides with varying numbers of nitroxide groups (one to four) derived from different aromatic core structures show intramolecular electron spin–spin coupling. The scope of this study is to establish an easy methodology for extracting structural, dynamical, and thermodynamical information from the EPR spectra of these polynitroxides which might find use as spin probes in complex systems, such as biological and host/guest systems, and as polarizing agents in dynamic nuclear polarization (DNP) applications. Density functional theory (DFT) calculations at the B3LYP/6-31G(d) level provided information on the structural details such as bond lengths and angles in the gas phase, which were compared with the single crystal X-ray diffraction data in the solid state. Polarizable continuum model (PCM) calculations were performed to account for solvent influences. The electron paramagnetic resonance (EPR) spectra of the polynitroxides in chloroform were analyzed in detail to extract information such as the percentages of different conformers, hyperfine coupling constants a , and rotational correlation times τ_c . The temperature dependence on the line shape of the EPR spectra gave thermodynamic parameters ΔH and ΔS for the conformational transitions. These parameters were found to depend on the number and relative positions of the nitroxide and other polar groups.



INTRODUCTION

Organic polyradicals are of critical importance in organic magnetism,^{1–3} molecular charge transfer,⁴ and multiple spin labeling in structural biology.⁵ The basis for bulk and molecular magnetic phenomena is the electron spin–spin exchange coupling between unpaired electrons localized on different centers. The correlation of this exchange coupling with structural parameters of the system of interest is a long-standing research topic.^{1–3}

Among organic radicals, nitroxides have the advantage that they are stable under ambient conditions and can be easily synthesized, manipulated, and derivatized. Polynitroxides have shown improved properties with respect to mononitroxides as organic ferromagnets, contrast agents in nuclear magnetic imaging, labels in electron magnetic resonance imaging, and radiation protectors during whole brain radiotherapy.⁶ When used as electron spin agents for dynamic nuclear polarization (DNP), polynitroxides can enhance the sensitivity of nuclear magnetic resonance (NMR) signals by orders of magnitude.⁷

The intramolecular spin exchange in polynitroxides has been investigated extensively, and a wide literature exists about the theory and analysis of their electron paramagnetic resonance (EPR) spectra.^{1–3,8–12} Such exchange coupling can be either ferromagnetic or antiferromagnetic, depending upon the topology and conformation of the coupling pathway connecting the radicals.^{1–3,13,14} Rigid polynitroxide scaffolds, which are too

constrained to allow intramolecular nitroxide collisions, can show spin exchange coupling by through-bond and/or through-space mechanisms.¹⁵ In general, for rigid polynitroxides with an aromatic backbone, the exchange coupling is mediated more effectively by through-bond interactions, especially through a cross-conjugated π -system.^{13,15} However, in solution, a through-space spin–spin exchange may be promoted by the solvent and other molecules in the nitroxide microenvironment.¹²

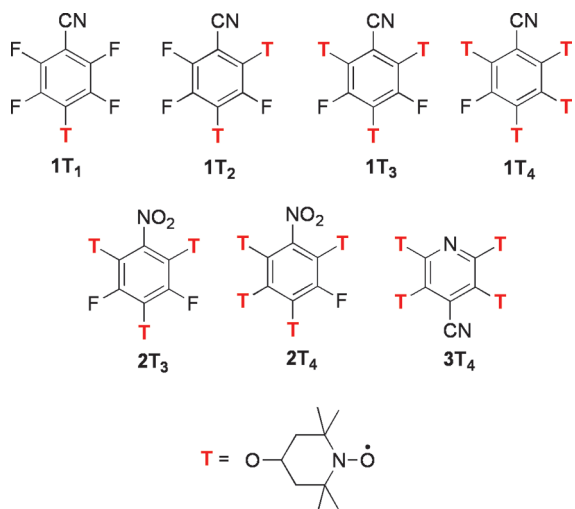
Most of the studies reported in the literature demonstrate the importance of coupling the EPR analysis of polynitroxides with structural and geometric analysis, such as X-ray diffraction analysis and computational studies. Recently, we reported a synthetic method based on nucleophilic aromatic substitution on electron-deficient aromatic compounds which yielded a series of polynitroxides exhibiting strong electron exchange between the radicals.¹⁶ We also reported single crystal X-ray diffraction analysis and basic EPR spectra of these polynitroxides.

In the present study we performed a computer-aided analysis of the EPR spectra, following a simplified procedure, for the series of polynitroxides shown in Scheme 1. These radicals were selected on the basis of different structural features, such as the

Received: July 6, 2011

Revised: December 1, 2011

Published: December 01, 2011

Scheme 1. Structures of the Investigated Polynitroxides

number of nitroxide groups (one through four), different aromatic backbones (cyanobenzene, nitrobenzene, or pyridine), and different relative positions of the nitroxide groups (vicinal or separated by groups with different polarities). The EPR analysis as a function of temperature led to the determination of thermodynamic parameters for intramolecular conformational transitions. To evaluate both the relative energies of various conformers and the hyperfine constants for the coupling between the electron spin and the ¹⁴N nuclear spin, we have optimized the gas-phase geometries of the polynitroxides with B3LYP/6-31G(d) calculations. The effects of a solvated (chloroform and water) environment were evaluated with the polarizable continuum model (PCM). A simple way of analyzing the EPR spectra of these polynitroxides is necessary for their use as spin probes of microenvironments and complex systems.

■ EXPERIMENTAL SECTION

The investigated polynitroxides (Scheme 1) were synthesized according to our previously published procedure.¹⁶ For the EPR analysis, solutions of polynitroxides in chloroform were prepared at a concentration of 0.1 mM. The solvent and concentration were selected on the basis of a good compromise between solubility and the reported effect on the spin–spin exchange interaction.¹² The solutions in 2 mm (inner diameter) quartz tubes were deoxygenated by six freeze–pump–thaw cycles.

X-band EPR spectra were acquired on an EMX-Bruker spectrometer. The sample temperature was controlled with a Bruker ER4131VT variable temperature accessory. The estimated accuracies of the measured ΔH and ΔS values are 0.1 kJ mol⁻¹ and 0.5 J mol⁻¹ K⁻¹, respectively.

Calculations of the gas-phase structures were performed with the Gaussian 09 set of programs.¹⁷ The total energies of the optimized geometries and the hyperfine coupling constants were obtained with the density functional theory (DFT) method using Becke's three parameter hybrid functional (B3),¹⁸ combined with the correlation functional of Lee, Yang, and Parr¹⁹ (LYP), with the standard 6-31G(d) basis set, using the unrestricted formalism for the open-shell species. The effects of a solvated environment were evaluated with the polarizable continuum model (PCM).

■ RESULTS AND DISCUSSION

Calculated Structures and Hyperfine Coupling Constants.

The optimized geometries, corresponding to the minima in the electronic potential energies, of the isolated polynitroxide molecules (Scheme 1) were obtained with B3LYP/6-31G(d) calculations. Some results are represented in Figure 1 and compared with previously reported¹⁶ X-ray crystal structures. The first column of Figure 1 displays representations of the most stable gas-phase conformers found by the calculations, the conformations reported in the central column are calculated to lie at higher energies (see below), and the third column displays the corresponding solid-state X-ray structures.¹⁶

For the mononitroxide 1T₁ the calculations found two local minima very close in energy, corresponding to the conformers represented in Figure 1, with the less stable lying at only 0.60 kJ/mol higher energy. The calculated gas-phase geometry parameters are compared with the solid-state counterparts in Table 1. The main difference between the geometry of the most stable conformer and the X-ray structure (last column of Figure 1) consists of different rotational angles of the piperidine ring around the two C–O bonds. According to the calculations, rotations around both these bonds cause only small energy changes (even in the polysubstituted analogues, except for the presence of piperidine rings adjacent to each other), so the optimized geometry lies in a shallow potential energy well. The solid-state conformation is therefore expected to be mainly determined by intermolecular interactions. These results indicate that the gas-phase calculation is probably more suitable than the solid-state structures to provide information on the conformations in solution, owing to the geometric effects caused by formation of a crystal lattice.

The dinitroxide 1T₂ bears piperidine substituents in ortho and para positions to the cyano group. The calculated optimized geometry is quite similar to the X-ray structure¹⁶ determined in the solid state (see Figure 1), with the two piperidine rings pointing in opposite directions relative to the benzene plane. However, a local energy minimum at only 2.03 kJ/mol higher energy (see Table 2) is found for a conformer where the two radicals are oriented toward the same side of the benzene ring. In both conformers the calculated N–O bond distances (1.285 Å), which are directly correlated to the coupling constants measured by EPR, are equal for both N–O groups and also the same as in the monosubstituted derivative 1T₁. All other bond lengths and angles are also very similar to the corresponding parameters of 1T₁.

Two close-in-energy local minima were calculated for the trinitroxide 1T₃, where the three radicals substitute the benzene positions 2, 4, and 6 (so that there are no vicinal substituents). The corresponding conformers are displayed in Figure 1. The conformer with the *p*-piperidine ring oriented in the opposite direction relative to the two ortho substituents (i.e., a conformation similar to that found in the solid state¹⁶) is predicted to be the most stable, but the conformer with all three radicals oriented toward the same side of the benzene plane is calculated to be only 2.61 kJ/mol less stable, in line with the results found in 1T₂. The B3LYP calculations predict similar conformers and energy difference (2.51 kJ/mol) for the nitro analogue 2T₃.

In tetranitroxide 1T₄ the four nitroxide substituents occupy the 2, 4, 5, and 6 positions of the benzene ring, so there are three vicinal radicals. According to the calculations, in the most stable conformer the substituents in positions 2 and 5 lie below the

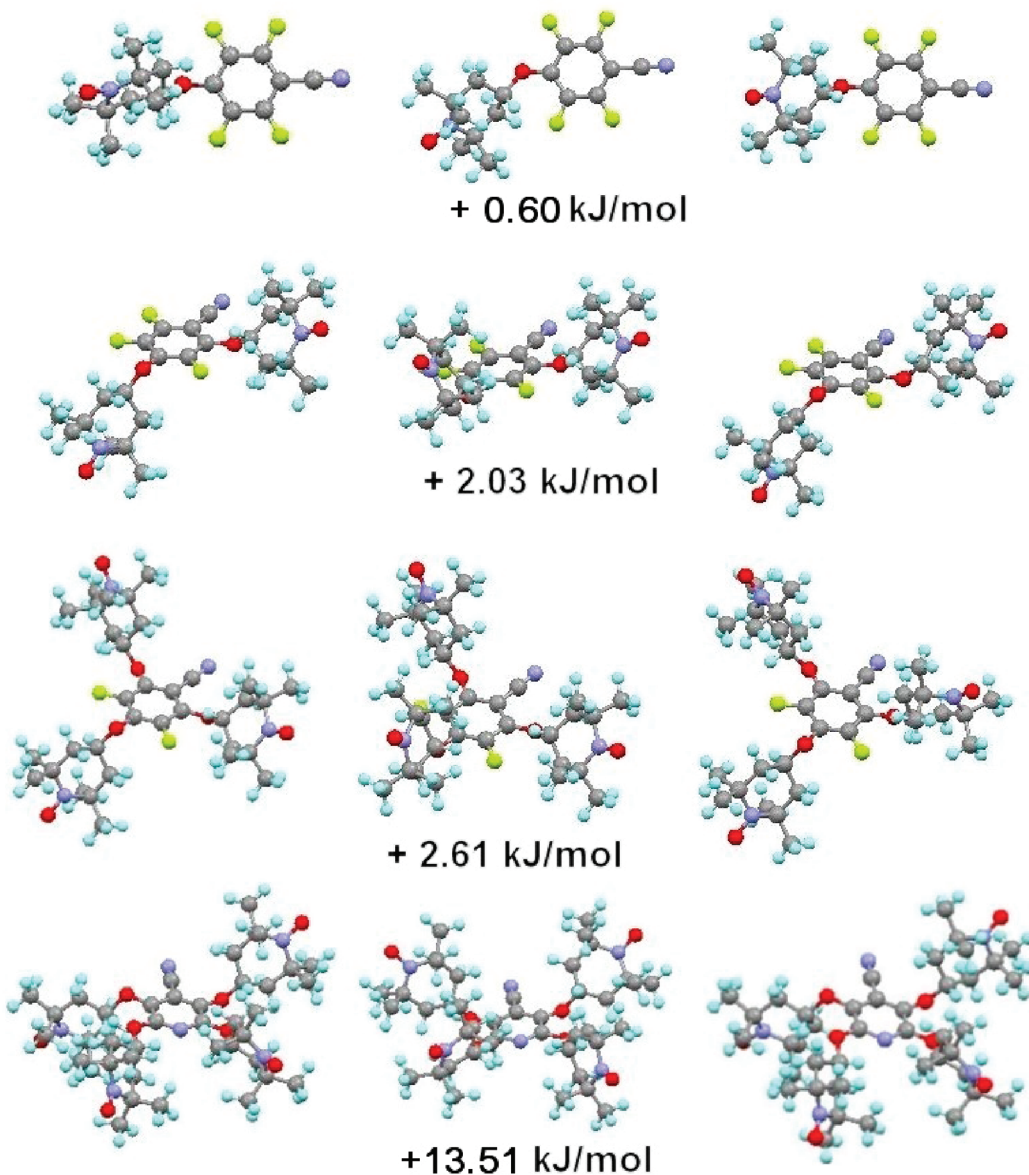


Figure 1. Representation of the most stable and other (see text) gas-phase conformations supplied by B3LYP/6-31G(d) calculations, and structures determined by single crystal X-ray diffraction¹⁶ of compounds 1T₁, 1T₂, 1T₃, and 3T₄.

benzene ring, with the two substituents in positions 4 and 6 pointing in the opposite direction. However, a conformer where only the radical in position 5 is oriented downward possesses an energy only slightly higher (0.87 kJ/mol), whereas a local minimum corresponding to a conformer where only the radical in position 4 is oriented downward (with the vicinal radicals in positions 5 and 6 both oriented upward) lies at sizably higher energy (30.39 kJ/mol). In all conformers, the four N–O distances (1.285 Å) are again predicted to be equal to each other and equal to those calculated for the smaller analogues. The calculations do not find any local energy minimum corresponding to a conformer with all four radicals oriented on the same side of the benzene ring.

For the nitro analogue 2T₄ the calculations predict a small energy difference (1.74 kJ/mol) between the two most stable conformers (corresponding to those found in the 1T₄ cyano counterpart). In this case, however, a local minimum is found also

for a conformer with all four radicals oriented on the same side of the benzene ring. Its energy is calculated to be sizably higher (57.12 kJ/mol, see Table 2) than that of the most stable conformer, in line with the occurrence of steric hindrance between three vicinal radicals. In all conformers the N–O distances (1.2846 Å) are calculated to be the same as in the 1T₄ analogues.

Finally, as shown in Figure 1, the most stable conformer of pyridine tetranitroxide 3T₄ looks quite similar to that found in the solid state.¹⁶ The calculations also find two more local minima at energies only slightly higher (0.02 and 2.99 kJ/mol). The N–O bond lengths (1.285 Å) are predicted to remain unchanged even in the various conformers of this pyridine derivative. No local energy minima are found by the calculations for conformers with all four radicals on the same side of the pyridine ring. One of these conformations, displayed in the central column of Figure 1, obtained by fixing at arbitrary values the four dihedral angles (and optimizing the remaining

Table 1. Bond Lengths (\AA) and Main Angles Calculated for the Two Most Stable Conformers (A and A', in Order of Increasing Energy) of 1T_1 and Corresponding Parameters Measured by Single Crystal X-Ray Diffraction

	gas phase (calcd)		
	A	A'	crystal
N–O	1.284	1.284	1.288
N–C (piperidine)	1.502	1.502	1.495
C–CN	1.424	1.425	1.438
C≡N	1.163	1.162	1.139
C–F	1.337	1.336	1.338
C _{Bz} –O	1.343	1.352	1.358
O–C _{pip}	1.459	1.461	1.473
COC (deg)	122.58	118.33	114.88
dih Bz ring~OC _{pip} ^a (deg)	24.57	63.93	84.29

^a Dihedral angle between the benzene ring and the O–C (piperidine) bond.

parameters), was calculated to lie at 13.51 kJ/mol higher energy than the most stable conformer. It can be noted that this energy difference is relatively small when compared to that (about 57 kJ/mol, as mentioned above) of the corresponding conformer of 2T_4 , where three vicinal radicals are present.

As a general result, the calculations indicate that rotations of the radical substituents around both C–O bonds cause only small energy differences, provided steric hindrance between vicinal rings is avoided. Moreover, the N–O bond distance is found to remain essentially constant ($1.2845 \pm 0.0001 \text{\AA}$), regardless of the number of radical substituents, conformation, and nature of the central benzenoid ring.

PCM calculations were carried out to evaluate the effects of solvents (water and chloroform) on the geometric parameters and hyperfine coupling constants. With both solvents the calculations found local minima corresponding to conformations very close to those calculated for the isolated molecules (gas phase). In all compounds, the N–O bond distances were predicted to increase from 1.2845\AA (gas phase) to about 1.2855\AA in chloroform and 1.2861\AA in water.

Table 2 reports the B3LYP/6-31G(d) hyperfine coupling constants calculated in the gas phase, water, and chloroform for the most stable conformer of each compound and a conformer with the nitroxide groups all oriented toward the same side of the aromatic ring. The (gas-phase) relative energies of the higher-lying conformers are also given. Water molecules were used to account for a polar environment leading to dipole–dipole interactions or, eventually, hydrogen bonding with the nitroxide groups. The optimized conformations resulted to be only slightly affected by both solvents, while (as mentioned above) the N–O bond distances were found to increase significantly on going from the gas phase, to chloroform, to water. Although this geometric change would act in the opposite direction, the coupling constants are calculated to be larger in the presence of solvent (about 3% in water, 2% in chloroform) than in the gas phase. The computed coupling constants given in Table 2 were used as starting values for the computation of the EPR spectra, as described in the following section.

Analysis of the EPR Spectra. The spin Hamiltonian for a biradical can be described by⁸

$$\begin{aligned} H = & g\beta_e B(S_z^{(1)} + S_z^{(2)}) + a(S_z^{(1)} \cdot I_z^{(1)} + S_z^{(2)} \cdot I_z^{(2)}) \\ & + J(S_z^{(1)} \cdot S_z^{(2)}) \end{aligned}$$

Table 2. B3LYP/6-31G(d) Hyperfine Coupling Constants (a , in Gauss) for the Most Stable Conformer and a Conformer with All the Nitroxide Groups Oriented toward the Same Ring Side^a

	ring position	a (G)		
		gas phase	water	chloroform
1T ₁	4	13.95	14.36	14.24
1T ₂	2	7.00	7.21	7.14
	4	6.98	7.23	7.15
1T ₂ , 2.03 kJ/mol less stable	2	7.00	7.20	7.13
	4	6.99	7.19	7.11
1T ₃	2	4.68	4.81	4.76
	4	4.66	4.80	4.75
	6	4.67	4.80	4.76
1T ₃ , 2.61 kJ/mol less stable	2	4.67	4.82	4.74
	4	4.65	4.79	4.73
	6	4.65	4.78	4.74
2T ₃	2	4.67	4.81	4.76
	4	4.66	4.79	4.75
	6	4.67	4.80	4.74
2T ₃ , 2.51 kJ/mol less stable	2	4.68	4.81	4.76
	4	4.65	4.79	4.74
	6	4.64	4.78	4.75
1T ₄	2	3.50	3.60	3.57
	4	3.50	3.60	3.56
	5	3.50	3.60	3.56
	6	3.49	3.60	3.56
2T ₄	2	3.51	3.59	3.57
	4	3.49	3.59	3.56
	5	3.49	3.59	3.55
	6	3.49	3.60	3.55
2T ₄ , 57.12 kJ/mol less stable	2	3.50	3.59	3.56
	4	3.53	3.62	3.58
	5	3.48	3.58	3.54
	6	3.50	3.60	3.56
3T ₄	2	3.50	3.60	3.56
	3	3.51	3.60	3.56
	5	3.51	3.60	3.56
	6	3.50	3.60	3.56
3T ₄ ^b , 13.51 kJ/mol less stable	2	3.49	3.58	3.55
	3	3.51	3.62	3.58
	5	3.48	3.63	3.58
	6	3.50	3.60	3.58

^a The energies relative to the most stable conformer (evaluated in the gas phase) are also reported. ^b Geometries optimized with (arbitrarily) fixed CCOC dihedral angles (2, 114°; 3, 155°; 5, -151°; 6, -119°).

where the first component is the Zeeman coupling between the unpaired electron spin and the magnetic field, the second component is the hyperfine coupling between the electron spin and the nitrogen nuclear spin ($I = 1$ for a nitroxide-¹⁴N radical; a is the hyperfine coupling constant between the electron spin and the nuclear spin), and the third component is the exchange coupling between the two electron spins (J is the exchange coupling constant). For the nitroxide biradical, two limiting cases are possible: (i) $a > J$ (J may be approximated to 0), where each

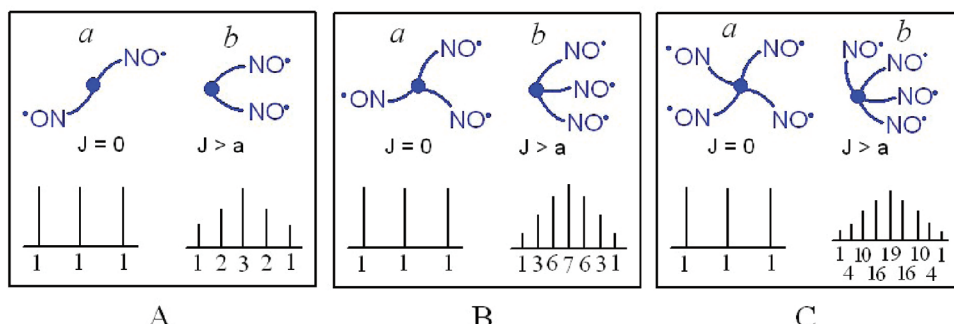


Figure 2. Schematic representation of slow exchange between two conformations (a, “far” conformation, with residence time τ_a ; b, “close” conformation, with residence time τ_b) providing a two-component spectrum: (A) binitroxide; (B) trinitroxide; (C) tetranitroxide.

nitroxide separately contributes to the EPR signal which is therefore constituted of three lines (number of lines = $2I + 1$) corresponding to the nuclear configurations $I^{(1)} = I^{(2)} = -1, 0, +1$ with relative intensities of 1:1:1; (ii) $J > a$, that is, each electron interacts equally with the two nitrogen nuclei; in this latter case the spectrum consists of five lines with relative intensities 1:2:3:2:1, as schematically represented in Figure 2A for a binitroxide as 1T₂. Analogously, the trinitroxides 1T₃ and 2T₃ present the same pattern in terms of number and position of lines. However, in these cases we are potentially dealing with three different J values, J_{12} , J_{23} , and J_{13} , corresponding to three different spin–spin interactions between the three nitroxides of the molecule. In the absence of spin–spin interactions, i.e., $J_{12} = J_{23} = J_{13} = 0$, the resulting spectrum is the typical three-line spectrum, whereas for $J_{12} \sim J_{23} \sim J_{13} > a$ a seven-line spectrum is expected with relative intensities of 1:3:6:7:6:3:1 (shown schematically in Figure 2B). Similarly, for the tetranitroxides 1T₄, 2T₄, and 3T₄ (Scheme 1), the simplest model, shown schematically in Figure 2C, is composed of two configurations, one with $J = 0$ and the other with all $J > a$. For the latter, nine lines with relative intensities of 1:4:10:16:19:16:10:4:1 are expected.

As reported in the literature,^{1h,8a,12,13,15} a through-space spin exchange mechanism between the nitroxide units is expected to give rise to the two limiting cases $J = 0$ and $J > a$, associated with a slow (in the EPR time scale) conversion between a “far” and a “close” conformation, as schematically shown in Figure 2. The “far” conformation (labeled “a” in Figure 2), with a residence time τ_a , does not allow the nitroxide groups to interact, whereas in the “close” conformation (“b” in Figure 2), with a residence time τ_b , the nitroxide groups approach each other and exchange their spin. The assumption of a single “close” conformation, with all the nitroxides approaching each other, is an approximation, useful for simplifying the EPR analysis. However, it is reported in the literature,^{1h,8a,12a,13,15} that rigid polynitroxides show an indirect through-bond spin exchange mechanism working via electron spin density delocalization over atoms and bonds in the bridge. The investigated polynitroxides are relatively rigid and contain an aromatic ring, which might allow spin exchange through the cross-conjugated π -system. However, it has also been reported^{1h,12,15b} that rigid polynitroxides may show a through-space spin exchange mechanism mediated by solvent molecules and interactions between differently polar moieties. Therefore, both through-space and through-bond spin exchange mechanisms may take place in the investigated polynitroxides.

With the purpose of using these polynitroxides as spin probes in complex systems of biological and environmental interest,

mainly host/guest systems, we exploit an easy spectral analysis approach for extracting structural, dynamical, and thermodynamical information on these radicals in solution. Therefore, we used an easily available and simple simulation procedure to compute the EPR line shape, just to reconstruct the experimental spectra and to obtain some useful information and parameters about these systems to be used in a comparative way.

First, we consider the spectra as a combination of the two limiting cases of $J = 0$ (“far” conformation) and $J > a$ (“close” conformation), as expected for nitroxides communicating through space. As shown in Figure 3, for 1T₂, the spectrum is clearly constituted by a three-line component and two lines in between, which belong to a five-line component. Similarly, for the trinitroxides 1T₃ and 2T₃, and for the tetranitroxides 1T₄, 2T₄, and 3T₄ a seven-line multiplet and a nine-line multiplet were found, respectively, superimposed to a three-line component. For the five-, seven-, and nine-line multiplets we verified that the number of lines and their positions did not change with temperature, thus indicating that the $J > a$ limiting case holds.⁸ Therefore, these experimental observations are consistent with the occurrence of a slow exchange between two conformations. The first step of the spectral analysis was the computation of the line shapes. This was accomplished either by adding a computed three-line signal (for the $J = 0$ configuration) to a computed multiplet of lines (for the $J > a$ configuration), or by adding Lorentzian lines at different intensities. Both methods allow the evaluation of the relative intensities of the “far” and “close” components and the hyperfine coupling constants, a . To extract the coupling constants, we started from the theoretical values listed in Table 2 and optimized the a values until experimental and computed spectra matched. We found an increase in the a values from the theoretical (gas-phase) values to the experimental (liquid-phase) values, which is expected if the NO group is in a more polar environment.²⁰ In spite of the rigidity of the molecular structure, the presence of polar bonds, such as C–F and C–N, may differently affect the solvation and the environmental polarity of each nitroxide group. For instance, the calculated distance between an NO group and a vicinal fluorine atom is about 7 Å, sufficiently small to influence the solvent distribution and the environmental polarity of the nitroxide group. Similarly, the distance between the CN and NO groups is about 5 Å, which is enough to promote solvent mediated dipole–dipole interactions. These interactions might promote through-space spin–spin interactions.¹²

For each polynitroxide, we describe first the computation performed by calculating separately the “far” and “close”

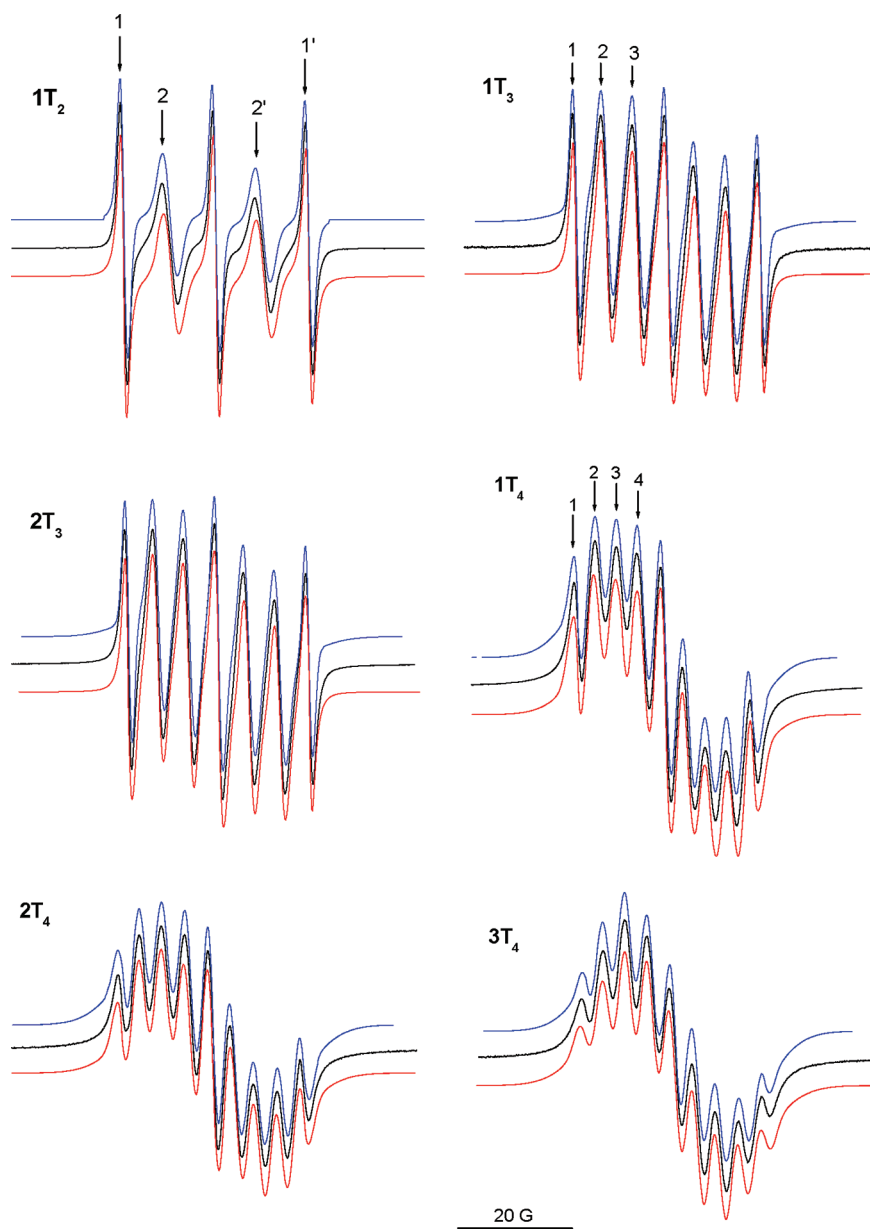


Figure 3. Experimental (black lines) and computed (red lines, sum of computed “close”, “far”, and “broad” components; blue lines, sum of Lorentzian lines) EPR spectra of the polynitroxides (0.1 mM) in CHCl_3 at 298 K.

components as multiplets of lines and then adding them to each other to reproduce the experimental line shapes. These computations are presented as red lines in Figure 3. The percentage of the “close” component for each polynitroxide is listed in Table 3. In these cases, we used both the program SimFonia (Bruker) and the program by Budil et al.,²¹ the latter was employed to compute the three-line signals. The method by Budil et al. presents the advantage of providing further information, such as the correlation times for rotational diffusion of the radicals, τ_c and accurate coupling constant values (with an estimated accuracy of 1–2% for all parameters). The hyperfine coupling constants and their averaged values $\langle a \rangle$, obtained with the SimFonia program in the computations of the “close” components, are listed in Table 3.

For 1T_2 in CHCl_3 at room temperature (298 K) the attempt to compute the line shape by adding two components (Figure 3, red line) was accomplished following the procedure already used

in a previous study.²² We added the three-line component to a two-line component using the Budil et al. program. Considering that the two-line component is part of the five-line spectrum of the “close” configuration with relative intensities of 1:2:3:2:1, the relative population of the “close” component was determined by double integration to be 72%. The “far” configuration (three-line spectrum) contributed 28% to the experimental spectrum. These values may be correlated to the time (τ_a or τ_b) spent by the system in each of the two configurations (“far” and “close”). As mentioned above, according to the calculations a local energy minimum at only 2.03 kJ/mol higher energy relative to the most stable conformer of 1T_2 corresponds to a conformer where both radicals are oriented toward the same side of the benzene ring (see Figure 1). The energy difference calculated in chloroform is further reduced to 1.74 kJ/mol, leading to a prediction (Boltzmann distribution) of about 50% of this conformer at

Table 3. Percentage of “Close” and “Broad” Components (Accuracy ± 0.5) and Hyperfine Coupling Constants (Gauss, Accuracy ± 0.05) for the EPR Spectra at 298 K of the Various Polynitroxides, As Obtained from Computation

sample	close ^a (%)	a_{ii} , close (G)	$\langle a \rangle$, close (G)	broad ^b (%)
1T ₂ -CHCl ₃	72	2N, 7.85	7.85	10
1T ₂ -H ₂ O/CH ₃ OH	40	2N, 8.35	8.35	25
1T ₃ -CHCl ₃	87	3N ($I = 3$), 5.25	5.25	31.5
2T ₃ -CHCl ₃	90	2N ($I = 2$), 5.1; 1N, 5.85	5.35	30
2T ₃ -H ₂ O/CH ₃ OH	54	3N ($I = 3$), 5.42	5.42	46
1T ₄ -CHCl ₃	83	1N, 3.0; 2N ($I = 2$), 3.9; 1N, 4.6	3.85	52
2T ₄ -CHCl ₃	92	1N, 3.15; 2N ($I = 2$), 3.9; 1N, 4.65	3.9	52
3T ₄ -CHCl ₃	100	2N ($I = 2$), 3.7; 2N ($I = 2$), 4.15	3.92	73

^a Percentage of the sum (close + far). ^b Percentage of the total.

298 K. Even if this conformer cannot be identified with the “close” configuration, the approaching of the nitroxide groups to each other to promote a through-space spin–spin coupling is favored by the solvent, but further attractive effects from other polar groups in the molecules, and/or a contribution from the through-bond coupling must be invoked to justify the high percentage of “close” component.

Therefore, we hypothesize that the high percentage of the “close” component may be caused by at least three different sources: (i) the solvent effect, that is, attractive/repulsive forces between the solvent molecules and the nitroxide groups, which enhance the stability of the “close” conformation in solution; (ii) dipole–dipole interactions between NO groups and vicinal polar groups (as such as F, CN, NO₂, and the pyridine nitrogen); (iii) an enhanced exchange coupling by a through-bond mechanism. Indeed, experiments performed in a more polar solvent (the experimental and computed spectra of 1T₂ in water/methanol = 1/1 at 298 K are shown in Figure S1a in the Supporting Information, while the main parameters used for computation are listed in Table 3) provided a much smaller percentage (40%) of five-line component, thus suggesting that the solvent plays a significant role on the exchange mechanism, which is in agreement with previous studies.¹²

Finally, inclusion of a further component was required to reproduce more satisfactorily the experimental line shape. A broad single line (width of about 20 G) was added with a 10% spectral contribution to the “far” and “close” components to reproduce the experimental line shape of 1T₂ in CHCl₃ at 298 K. In water/methanol (Table 3) this percentage increases to 25% at the same temperature, and it also increases by decreasing the temperature. About the same ratio between the three components—“far”, “close”, and “broad”—was found for the spectra in water/methanol at 298 K and in chloroform at 250 K; the temperature effect on the line shape is visually evident, as shown in Figure 4 for 2T₃. Therefore, this broad component may be ascribed to self-aggregated radicals, due to solubility problems of the polynitroxides in the solvents as a function of polarity and temperature. The signal broadening is also affected by radical concentration: an increase in concentration provokes line broadening due to intermolecular spin–spin interactions, whereas a decrease in concentration increases the signal noise and therefore decreases the accuracy in the spectral analysis.

The computation of the three-line component (“far” configuration) for 1T₂ in CHCl₃ gave a correlation time for the rotational diffusion $\tau_c = 0.026$ ns, which is characteristic of a fast tumbling of the radicals in solution, at low microviscosity. This computation also provided a hyperfine coupling constant of $\langle a \rangle = 15.75$ G. Both mobility and polarity parameters increase

from chloroform to water/methanol (Figure S1a, Supporting Information), which is in agreement with a higher microviscosity and polarity of water/methanol with respect to chloroform. The polarity variation is also in agreement with the variation of the hyperfine coupling constant from CHCl₃ to water obtained by B3LYP calculations.

The coupling constant for the $J > a$ case (e.g., the “close” component) is about half that for the $J = 0$ case, that is, 7.85 G. The corresponding B3LYP/6-31G(d) value in chloroform (7.15 G, see Table 2) is underestimated by about 9–10%. Although this difference could in part arise from inadequacy of the theoretical model, it seems plausible to ascribe it mainly to the above-mentioned effects related to interactions with the neighboring solvent molecules or substituents of different polarities, such as CN, NO₂, and F.

The experimental spectra of 1T₃ and 2T₃ in chloroform at 298 K (Figure 3, black lines) were computed (Figure 3, red lines) by adding two contributions, a three-line and a seven-line signal, plus a contribution from a broad component, as described for 1T₂.

Conveniently, for 1T₃, the seven-line signal could be simulated considering the three nitrogens as a single nucleus with $I = 3$. This provided the same relative intensities of the seven lines. The simulation by means of an $I = 3$ nucleus is a suitable approximation which may account for a strong spin exchange, as also suggested by the high relative percentage of the seven-line component (87%, Table 3).

In the case of 2T₃ the computation of the seven-line component was performed by means of an $I = 2$ nucleus and an $I = 1$ nucleus, with quite different a values ($a(I=2) = 5.1$ G; $a(I=1) = 5.85$ G; Table 3). The percentage of the close component increased from 1T₃ to 2T₃ (Table 3), in line with the not negligible decrease in the energy gap between the stable and the “total-up” conformation for 2T₃ with respect to 1T₃, obtained by B3LYP calculation (Table 2). Of course we cannot exclude that different choices of I and a values can also reproduce the line shape. However, the $I > 1$ approximation may be used as an indicator of the simultaneous contributions of through-bond and through-space spin–spin exchange interactions, which is a matter largely debated in the literature,^{1,12–15} whereas the different a values account for attractive and repulsive interactions between the nitroxide groups and other molecules and polar groups at the nitroxide microenvironment. For instance, the highly polar C–F group may be responsible for an increase in environmental polarity of the neighboring nitroxide group, mediated by the solvent. In any case, the results indicate that the spectra of 2T₃ are more informative about environmental modifications affecting the spin–spin exchange process with

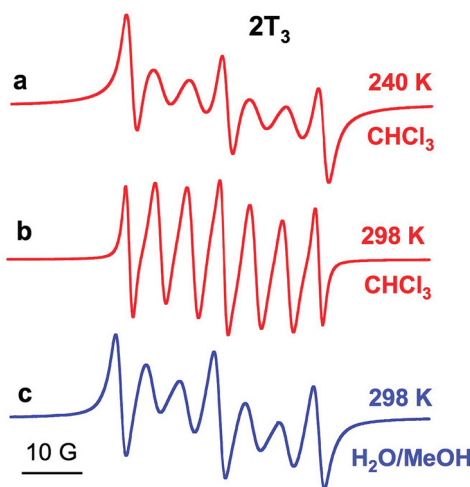


Figure 4. Experimental EPR spectra of 2T₃ (0.1 mM) in chloroform (a, b) and water/methanol = 1/1 (c) at 240 K (a) and 298 K (b, c).

respect to those of 1T₃. These results, together with the higher percentage of “close” component, indicate that the former is a better candidate to be used as a spin probe in complex systems.

The computation of the three-line component for 1T₃ and 2T₃ in the “far” conformation provided a rotational mobility ($\tau_c = 0.026$ ns) which is the same as that found for 1T₂, indicating that addition of a third nitroxide group in the ortho position does not alter the possibility of free rotation.

For the computation of the trinitroxide spectra, the starting hyperfine coupling constants were those obtained from B3LYP calculations (4.75 G in chloroform). As found for 1T₂, to compute the EPR spectra, we increased this value to 9–10% which accounts for further polarity variations in the N–O environment due to neighboring polar groups (as such as CN, F, and NO₂). From the computation of the EPR spectra, the averaged coupling constant for the seven-line component was 5.25 G for 1T₃ and 5.35 G for 2T₃, thus indicating that the nitroxide–environment interactions cause a coupling constant increase of about 10% for 1T₃ and about 11% for 2T₃. The coupling constant for the three-line component was 15.75 G, that is, about 3 times that of the seven-line component.

To investigate solvent effects on the EPR spectra of 2T₃, additional experiments in a water/methanol mixture (1:1) were performed. The EPR spectrum in water/methanol (Figure 4c; see also Figure S1b in the Supporting Information for the computation) shows significant differences compared to the spectrum in chloroform (Figure 4b; compare the parameters in Table 3), as follows:

- A. A relative decrease of the percentage of the “close” component with respect to the “far” one is observed, even if according to the B3LYP calculations the energy gap between the stable and the “up” conformations is smaller in water than in chloroform. This seems to indicate that water, on one side, favors the energy stabilization of the close conformation but, on the other side, partially interrupts the through-space spin–spin communication between the nitroxides, as already found for other polynitroxides.¹²
- B. An increase in relative percentage of the broad component is observed, due to a decreased solubility in water with respect to chloroform.
- C. An increase of the hyperfine coupling constants, due to the increased environmental polarity in water, and a decreased

rotational mobility of the nitroxides, due to the increased microviscosity, are observed.

- D. The computation of the close component with the approximated “ $I > 1$ method” showed that 2T₃ in water/methanol needed an $I = 3$ nucleus (Table 3), instead of the $I = 2 + I = 1$ nuclei used for computing the spectrum in chloroform at 298 K. This is in line with an increase of a through-bond mechanism at the expense of a through-space one, due to the water effect on the through-space spin–spin communication.

Comparison of the EPR spectra of the three tetranitroxides 1T₄, 2T₄, and 3T₄ reveals interesting analogies and differences. The spectrum of 1T₄ in CHCl₃ at 298 K (Figure 3) was reproduced by adding 17% of a three-line component to 83% of a nine-line component (Table 3). Therefore the relative amount of the three-line component for 1T₄ was higher than that for 1T₃. This suggests that the additional nitroxide group inhibits the spin exchange. The computation of the nine-line component was accomplished by assuming a coupling with one nitrogen nucleus ($I = 1$) with $a = 3.0$ G, two nitrogen nuclei as a single nucleus ($I = 2$) with $a = 3.9$ G, and the fourth nitrogen ($I = 1$) with $a = 4.6$ G (Table 3). In this case too, as such as for 2T₃, it was chosen to use an $I = 2$ nucleus and significantly different a values to reproduce the experimental line shape, but this provides a convenient method to have a semiquantitative comparative evaluation of the occurrence of both through-space and through-bond spin–spin coupling. The proximity of different polar groups (C–F and C–CN) to the various NO moieties accounts for the different a values and may also favor the approaching of the nitroxide groups to each other.

On the basis of a significant increase in percentage of the broad component (as listed in Table 3; 31.5% for 1T₃ and 52% for 1T₄), the self-aggregation of 1T₄ is much higher than that of 1T₃.

For the spectrum of 2T₄ at 298 K (Figure 3) the best fitting between the computed and experimental line shapes was accomplished using parameters similar to those of 1T₄ (Table 3), but with a values somewhat larger, in agreement with a higher polarity and NO proximity of the NO₂ group with respect to the CN group. The NO₂ group also enhances the spin–spin exchange with respect to the CN group; in fact, the percentage of close component increases up to 92% (Table 3). While for 1T₄ the B3LYP calculations did not find an energy minimum for a conformer with the four radicals oriented toward the same side of the benzene plane, for 2T₄ a local energy minimum was located at 57.12 kJ/mol (52.1 and 47.1 kJ/mol, respectively, in chloroform and water) higher energy with respect to the most stable conformer. It can be noted that this large energy difference leads to the prediction that this conformation should not be populated at 298 K.

Finally, the spectrum of 3T₄ at 298 K (Figure 3) afforded the computation by means of a single component (in addition to the broad component due to low solubility), corresponding to a nine-line signal obtained considering two nitrogens as a single nucleus ($I = 2$) with $a = 3.7$ G and the other two nitrogens, again as a single nucleus ($I = 2$), with $a = 4.15$ G. The B3LYP calculations (Table 2) also indicated a much lower energy gap (13.51 kJ/mol) between the most stable and the “total-up” conformations with respect to 2T₄. The observed decrease of the three-line contribution on going from 1T₄ to 2T₄ and 3T₄ indicates an increasing exchange interaction among the NO groups along this series. However, the two couples of $I = 2$ nuclei

assumed for simulating the EPR line shape of $3T_4$ by means of our simplified computation method suggest that the through-bond communication is partially impeded between the two couples of nitroxide radicals.

Comparison of the experimental (averaged) hyperfine coupling constants ($1T_4$, 3.85 G; $2T_4$, 3.90 G; $3T_4$, 3.92 G) and the corresponding B3LYP values (3.56 G in chloroform, Table 2) indicates an increase in environmental polarity of 8, 10, and 10%, respectively, for $1T_4$, $2T_4$, and $3T_4$.

In summary, the hyperfine coupling constant determined from experimental spectra is consistently larger than that obtained from B3LYP calculations in chloroform, but interestingly, this increase is almost constant for all the polynitroxides (9–10%), being a little bit smaller for $1T_4$ and a little bit higher for $2T_3$. On the basis of a higher hydrophobic parameter (the partition coefficient between water and a hydrophobic immiscible solvent) of nitrobenzene ($\log P = 1.85$) with respect to benzonitrile ($\log P = 1.56$),²³ we expected higher a values (higher environmental polarity) in $2T_3$ and $2T_4$ than in $1T_3$ and $1T_4$ respectively.

The EPR spectra of the various polynitroxides in CHCl_3 at 298 K were also simulated with Lorentzian lines at the proper fields and relative intensities. Therefore we computed and added Lorentzian lines for each of the hyperfine lines constituting the “far” and “close” components, and finally a Lorentzian line reproducing the “broad” component was added, too. The results of these computations are displayed as blue lines in Figure 3, superimposed to the experimental spectra (black lines).

As described by Parmon and co-workers,⁸ in case the line position does not change with temperature, the relative intensities of the Lorentzian lines, calculated (double integration) for each radical as a function of temperature, may be used to evaluate the thermodynamic parameters ΔH and ΔS for the conversion between the “far” and the “close” conformations that contribute to the spectrum. As the temperature increases, the less stable conformation will be more populated. Figure 4a,b shows representative examples on how the EPR spectra change with changing temperatures. However, the line positions do not change. The arrows in the spectra in Figure 3 indicate the numbered hyperfine lines whose relative intensities are used for the calculation of the thermodynamic parameters, as described below.

For $1T_2$, whose spectrum was simulated (Figure 3, blue line) by adding five Lorentzian lines for the “far” and “close” components (we do not mention the broad component for all the polynitroxides because it is not used for the calculation of the thermodynamic parameters), first we verified that lines 1 and $1'$ as well as lines 2 and $2'$ are of the same doubly integrated intensity (results not shown). This symmetry in intensity between the right and left sides of the EPR spectra holds for all the polynitroxides, and therefore the calculations were performed using only one side (as such as lines 1 and 2 for $1T_2$).

Referring to Figures 2 and 3, the intensity of line 1, I_1^a , of the spectrum of $1T_2$ reflects the time, τ_a , spent in the “far” conformation ($J = 0$) over the total time of the measurements:

$$I_1^a = [\tau_a / (\tau_a + \tau_b)] [I/3]; \quad I_2^a = 0$$

The intensity of I_1^a is divided by 3, because the intensity of the first line is one-third of the total intensity I of the three-line component. The intensity of line 2, I_2^a , is 0 for the “far” conformation.

In the “close” conformation ($J > a$), indicated as “b” in Figure 2, the intensity of the first and second lines can be analogously

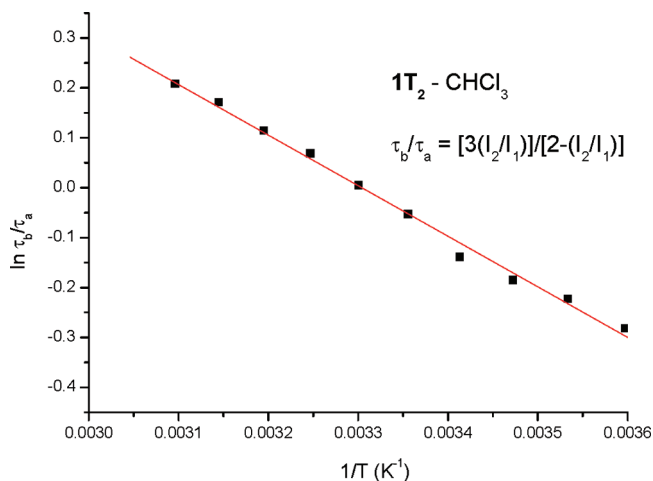


Figure 5. Arrhenius plot ($\log(\tau_b/\tau_a)$ vs $1/T$) for the transition from the far (residence time τ_a) to the close (residence time τ_b) conformation for $1T_2$. The intercept is $\Delta S/R$, and the slope is $-\Delta H/R$ (Table 4).

expressed as

$$I_1^b = [\tau_b / (\tau_a + \tau_b)] [I/9]; \quad I_2^b = [\tau_b / (\tau_a + \tau_b)] [I/3]$$

In this case, the first of the five lines is only one-ninth of the entire intensity, whereas the second line, having intensity 2, is one-third.

The total intensity of the first two lines at any given combination of the two cases is

$$I_1 = I_1^a + I_1^b = [(3\tau_a + \tau_b)/(\tau_a + \tau_b)] [I/9]; \\ I_2 = I_2^a + I_2^b = [\tau_b / (\tau_a + \tau_b)] [I/3]$$

From here

$$I_2/I_1 = 2\tau_b / (3\tau_a + \tau_b)$$

$$\tau_b/\tau_a = [3(I_2/I_1)]/[2 - (I_2/I_1)]$$

where, again, I_1 is the integrated intensity of the first (or fifth) line and I_2 is the integrated intensity of the second (or fourth) line. After repeating the Lorentzian lines fitting at several temperatures (T), plotting $\log(\tau_b/\tau_a)$ vs $1/T$ afforded the Arrhenius plot shown in Figure 5, whose intercept is $\Delta S/R$ and slope is $-\Delta H/R$, where the entropy and enthalpy changes are related to the conversion between “far” and “close” conformations, such as those sketched in Figure 2.

The Arrhenius plot (Figure 5) provides $\Delta H = 8.4 \text{ kJ mol}^{-1}$ and $\Delta S = 28 \text{ J K}^{-1} \text{ mol}^{-1}$, which is in agreement with previous data reported for “soft” biradicals in solution where the approaching of the two nitroxide moieties is partially hindered.⁸ In our case, we mainly refer to structural changes leading to different conformers, such as those identified by means of the B3LYP calculations. However, as discussed above, it is conceivable that the solvent effect and dipole–dipole interactions between vicinal polar groups in the radical structure will lead to a “close” conformation that is not feasible in the gas phase.

A similar procedure was repeated for the trinitroxides and tetranitroxides, using the intensities of the hyperfine lines indicated by arrows in Figure 3. The equations for the variation of

Table 4. Thermodynamic Parameters ΔH (kJ mol^{-1}) and ΔS ($\text{J mol}^{-1} \text{K}^{-1}$) for the Transitions between the “Far” and “Close” Conformations, Obtained from the Arrhenius Plots for the Different Polynitroxides and the Different Intensity Ratios between the Hyperfine Lines^a

radical	from I_2/I_1		from I_3/I_1		from I_4/I_1	
	ΔH	ΔS	ΔH	ΔS	ΔH	ΔS
$1T_2$	8.4	28				
$1T_3$	9.7	44	7.5	30		
$2T_3$	9.4	46	9.6	41		
$1T_4$	10.3	54.5	17	68.4	10	41
$2T_4$	9.7	54.6	12.7	57.5	8.7	42.7
$3T_4$	5.9	49	3.35	40	4.8	43

^a The accuracy in the thermodynamic parameters is about 3%.

the lifetime ratio between the “close” and “far” configurations for the trinitroxides and the tetranitroxides are derived in the Supporting Information, where also the Arrhenius plots are shown (Figure S2). The thermodynamic parameters obtained for the investigated polynitroxides are listed in Table 4.

The comparative analysis for all the polynitroxides on the basis of the data in Table 4 can be rationalized as follows:

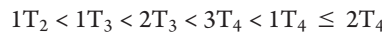
Both ΔH and ΔS are positive. $\Delta H > 0$ means that the transition from the “far” to the “close” conformation is endothermic and the “far” conformation is consequently more stable, in agreement with the B3LYP calculations. The meaning of $\Delta S > 0$ is less obvious and, as described in the literature,²⁴ is related to the complexity of the system.

For the trinitroxides $1T_3$ and $2T_3$ two different sets of thermodynamic parameters (Table 4) were obtained from the different intensity ratios, as such as from I_2/I_1 and I_3/I_1 in the spectrum of $1T_3$ in Figure 3. Indeed, the intensity ratio between I_2 and I_3 in the seven-line multiplet is expected to be 1:2; if this ratio is different, the resulting difference in the two τ_b/τ_a ratios at a certain temperature and the consequent difference in the thermodynamic parameters are due to a complex mechanism of exchange interaction which alters the relative intensities of the seven lines with respect to the expected 1:3:6:7:6:3:1. This is in line with the need for $I = 3$ and $I = 2$ nuclei in the computations of $1T_3$ and $2T_3$, as discussed above. Similarly, for the tetranitroxides, the different sets of thermodynamic parameters obtained from the different intensity ratios (Table 4) show discrepancies in line with the results obtained from computation and ascribed to the occurrence of both through-space and through-bond spin exchange mechanisms. However, the discrepancies between the two (for the trinitroxides) and the three (for the tetranitroxides) series of data (Table 4) might be caused by the assumption that only two conformations, “close” and “far”, are present. With increasing number of NO groups on the polynitroxide, intermediate conformations might alter the line shapes of the EPR spectra.

The ΔH values obtained from the I_2/I_1 intensity ratio for the various polynitroxides (see Table 4) increase in the following order: $3T_4 < 1T_2 < 2T_3 < 1T_3 = 2T_4 < 1T_4$. This trend indicates that $3T_4$ in “close” conformation (that is, possessing a strong spin exchange) is relatively more stable than the corresponding conformers of the other polynitroxides, with the most unstable “close” conformation being that of $1T_4$. This result is nicely in agreement with the B3LYP calculations (Table 2) which indicate

that the energy gap between the most stable conformer and the other one with all nitroxide groups on the same side is smaller for $3T_4$ with respect to the other tetranitroxides. This means that the pyridine ring of $3T_4$, together with a symmetric and less crowded distribution of the nitroxide groups, favors the approaching of the nitroxide groups to form the close conformation, with respect to the benzene-NO₂ and benzene-CN structures, the latter one being the most effective in impeding the approaching of the nitroxide groups. Consistently, $2T_3$ shows a slightly smaller transition enthalpy with respect to $1T_3$. These results are in agreement with the enhanced percentage of “close” components of the NO₂ derivatives revealed from the computation of the spectra (Table 3). However, in spite of the relatively low percentage of the “close” component, $1T_2$ shows a relatively lower energy barrier for the far-to-close transition with respect to the other polynitroxides, with the exception of $3T_4$. This means that the increase in the number of attached nitroxides decreases the stability of the close conformation. Also, the distribution of the nitroxide groups, symmetrically positioned at the benzene ring, plays an important role in the spin–spin interactions.

By comparing the values obtained from the I_2/I_1 intensity ratio for each radical (Table 4), the variation of ΔS for the different polynitroxides is as follows:



As expected on the basis of the meaning of ΔS described above, the ΔS values increase with the number of nitroxide substituents and with the size of the aromatic ring substituents.

CONCLUSIONS

The geometric structures of polynitroxides with varying numbers of nitroxide groups and varying structure of the backbone (with fluorine, cyano, and nitro groups) were calculated with the DFT method at the B3LYP/6-31G(d) level to obtain the energies of various conformers and the hyperfine coupling constants, in the gas phase and simulating solvent (water and chloroform) effects. The optimized geometries are in good agreement with single crystal X-ray diffraction data. The hyperfine coupling constants obtained with B3LYP calculations in conjunction with the PCM method to account for a chloroform environment were used as a basis for the computations of the experimental EPR spectra. An almost constant increase of 10% was found from the B3LYP constants to those needed for the EPR spectral computations.

The EPR spectra were analyzed considering only two limiting conformations, termed “close” and “far”, in line with a previously established methodology of analysis for dinitroxides. Parameters, such as coupling constants a and rotational correlation times τ_c , were obtained from an easy computational procedure, which give information about the micropolarity and microviscosity around the polynitroxides. This simplified EPR analysis provided interesting information on the spin–spin exchange process which can occur by through-bond and/or through-space mechanisms, the former through the cross-conjugated π -system, and the latter being mediated by the solvent and the polar groups of the radicals. In addition, thermodynamic parameters for the conformational transition (ΔH and ΔS) were extracted from the temperature dependence of the EPR spectra.

All the above information, which can be readily extracted from the present analysis approach, provided an overview of the properties of the polynitroxides in solution and are helpful to

select the best candidates to be used as spin probes in complex systems. Further studies are in progress, where supramolecular host–guest systems are investigated with these polynitroxides.

■ ASSOCIATED CONTENT

S Supporting Information.

S Supporting Information. Equations to evaluate the lifetime ratio between the “far” and the “close” configurations for the trinitroxides $1T_3$ and $2T_3$ and for the tetranitroxides $1T_4$, $2T_4$, and $3T_4$. Figure S1, experimental and computed (by adding a “far”, a “close”, and a “broad” component) EPR spectra of $1T_2$ (0.1 mM) (a) and $2T_3$ (b) in water/methanol (1/1) at 298 K. Figure S2, Arrhenius plots for the various tri- and tetranitroxides, calculated for different intensity ratios between hyperfine lines belonging to the close and far conformations. This material is available free of charge via the Internet at <http://pubs.acs.org>.

AUTHOR INFORMATION

Corresponding Author

*Tel.: +39 0722 304320. Fax: +39 0722304222. E-mail: maria.ottaviani@uniurb.it.

■ ACKNOWLEDGMENT

A.M. (University of Bologna) thanks the Italian Ministero dell'Istruzione, dell'Università e della Ricerca, for financial support. N.J.T. thanks the National Science Foundation, USA, for financial support through Grant NSF-CHE-0717518.

■ REFERENCES

- select the best candidates to be used as spin probes in complex systems. Further studies are in progress, where supramolecular host–guest systems are investigated with these polynitroxides.

■ ASSOCIATED CONTENT

S Supporting Information. Equations to evaluate the lifetime ratio between the “far” and the “close” configurations for the trinitroxides $1T_3$ and $2T_3$ and for the tetranitroxides $1T_4$, $2T_4$, and $3T_4$. Figure S1, experimental and computed (by adding a “far”, a “close”, and a “broad” component) EPR spectra of $1T_2$ (0.1 mM) (a) and $2T_3$ (b) in water/methanol (1/1) at 298 K. Figure S2, Arrhenius plots for the various tri- and tetranitroxides, calculated for different intensity ratios between hyperfine lines belonging to the close and far conformations. This material is available free of charge via the Internet at <http://pubs.acs.org>.

■ AUTHOR INFORMATION

Corresponding Author
*Tel.: +39 0722 304320. Fax: +39 0722304222. E-mail: maria.ottaviani@uniurb.it.

■ ACKNOWLEDGMENT

A.M. (University of Bologna) thanks the Italian Ministero dell’Istruzione, dell’Università e della Ricerca, for financial support. N.J.T. thanks the National Science Foundation, USA, for financial support through Grant NSF-CHE-0717518.

■ REFERENCES

 - (1) (a) Iwamura, H.; Koga, N. *Acc. Chem. Res.* **1993**, *26*, 346. (b) Ferruti, P.; Gill, D.; Klein, M. P.; Wang, H. H.; Entine, G.; Calvin, M. *J. Am. Chem. Soc.* **1970**, *92*, 3704. (c) *Magnetic Properties of Organic Materials*; Lahti, P. M., Ed.; Marcel Dekker: New York, 1999; pp 1–713. (d) *Molecular Magnetism*; Itoh, K., Kinoshita, M., Eds.; Kodansha: Tokyo, 2000; pp 1–337. (e) *Magnetic Molecular Materials*; Gatteschi, D.; Kahn, O.; Miller, J. S.; Palacio, F., Eds.; NATO ASI Series; Kluwer Academic Publishers: Dordrecht, 1991. (f) Yamaguchi, K.; Okumura, M.; Maki, J.; Noro, T.; Namimoto, H.; Nakano, M.; Fueno, T.; Nakasuiji, K. *Chem. Phys. Lett.* **1992**, *190*, 353. (g) Barone, V.; Bencini, A.; di Matteo, A. *J. Am. Chem. Soc.* **1997**, *119*, 10831. (h) Fritscher, J.; Beyer, M.; Schiemann, O. *Chem. Phys. Lett.* **2002**, *364*, 393.
 - (2) (a) Rajca, A.; Shiraishi, K.; Vale, M.; Han, H.; Rajca, S. *J. Am. Chem. Soc.* **2005**, *127*, 9014. (b) Rajca, A. *Adv. Phys. Org. Chem.* **2005**, *40*, 153.
 - (3) Fukuzaki, E.; Nishide, H. *J. Am. Chem. Soc.* **2006**, *128*, 996.
 - (4) (a) Weiss, E. A.; Tauber, M. J.; Kelley, R. F.; Ahrens, M. J.; Ratner, M. A.; Wasielewski, M. R. *J. Am. Chem. Soc.* **2005**, *127*, 11842. (b) Chernick, E. T.; Mi, Q.; Kelley, R. F.; Weiss, E. A.; Jones, B. A.; Marks, T. J.; Ratner, M. A.; Wasielewski, M. R. *J. Am. Chem. Soc.* **2006**, *128*, 4356.
 - (5) (a) Hustedt, E. J.; Beth, A. H. *Annu. Rev. Biophys. Biomol. Struct.* **1999**, *28*, 129. (b) Eaton, S. S.; Eaton, G. R. *Biol. Magn. Reson.* **2000**, *19*, 1. (c) Altenbach, C.; Oh, K.-J.; Trabanino, R.; Hideg, K.; Hubbell, W. *Biochemistry* **2001**, *40*, 15471. (d) Hanson, P.; Millhauser, G.; Formaggio, F.; Crisma, M.; Toniolo, C. *J. Am. Chem. Soc.* **1996**, *118*, 7618.
 - (6) (a) Kovarski, A. L.; Sorokina, O. N. *J. Magn. Magn. Mater.* **2007**, *311*, 155. (b) Crayston, J. A.; Devine, J. N.; Walton, J. C. *Tetrahedron* **2000**, *56*, 7829. (c) Hyodo, F.; Soule, B. P.; Matsumoto, K.; Matsumoto, S.; Cook, J. A.; Hyodo, E.; Sowers, A. L.; Krishna, M. C.; Mitchell, J. B. *J. Pharm. Pharmacol.* **2008**, *60*, 1049. (d) Fuchs, J.; Groth, N.; Herrling, J. *Biol. Magn. Reson.* **2003**, *18*, 483. (e) Metz, J. M.; Smith, D.; Mick, R.; Lustig, R.; Mitchell, J.; Cherakuri, M.; Glatstein, E.; Hahn, S. M. *Clin. Cancer Res.* **2004**, *10*, 6411.
 - (7) (a) Matsuki, Y.; Maly, T.; Ouari, O.; Karoui, H.; LeMoigne, F.; Rizzato, E.; Lyubenova, S.; Herzfeld, J.; Prisner, T.; Tordo, P.; Griffin, R. G. *Angew. Chem., Int. Ed.* **2009**, *48*, 4996. (b) Song, C.; Hu, K.-N.; Joo, C.-G.; Swager, T. M.; Griffin, R. G. *J. Am. Chem. Soc.* **2006**, *128*, 11385.
 - (8) (a) Parmon, V. N.; Kokorin, A. I.; Zhidomirov, G. M. Z. *Strukt. Khim.* **1977**, *18*, 132. (b) Parmon, V. N.; Kokorin, A. N.; Zhidomirov, G. M.; Zamaraev, K. N. *Mol. Phys.* **1975**, *30*, 695.
 - (9) Sankarapandi, S.; Rifkind, J. M.; Manoharan, P. T. *Proc.—Indian Acad. Sci., Chem. Sci.* **1994**, *106*, 1329.
 - (10) (a) Golubev, V. A.; Neiman, M. B.; Rozantsev, É. G.; Suskina, V. I. Z. *Org. Khim.* **1966**, *2*, 1916. (b) Luckhurst, G. R. *Mol. Phys.* **1966**, *10*, 543. (c) Glarum, S. H.; Marshall, J. H. *J. Chem. Phys.* **1967**, *47*, 1374. (d) Turro, N. J.; Khurdyakov, I. V.; Bossmann, S. H.; Dwyer, D. W. *J. Phys. Chem.* **1993**, *97*, 1138. (e) Corvaja, C.; de Narchi, M.; Toffoletti, A. *Appl. Magn. Reson.* **1997**, *12*, 1. (f) Hudson, A.; Luckhurst, G. R. *Mol. Phys.* **1967**, *13*, 409.
 - (11) Alster, E.; Silver, B. L. *Mol. Phys.* **1986**, *58*, 977.
 - (12) (a) Kokorin, A. I.; Tran, V. A.; Rasmussen, K.; Grampp, G. *Appl. Magn. Reson.* **2006**, *30*, 35. (b) Tran, V. A.; Rasmussen, K.; Grampp, G.; Kokorin, A. I. *Appl. Magn. Reson.* **2007**, *32*, 395.
 - (13) (a) Jacobs, S. J.; Shultz, D. A.; Jain, R.; Novak, J.; Dougherty, D. A. *J. Am. Chem. Soc.* **1993**, *115*, 1744. (b) West, A. P., Jr.; Silvermann, S. K.; Dougherty, D. A. *J. Am. Chem. Soc.* **1997**, *119*, 1452. (c) Shultz, D. A.; Bodnar, S. H.; Lee, H.; Kampf, J. W.; Incarvito, C. D.; Rheingold, A. L. *J. Am. Chem. Soc.* **2002**, *124*, 10054. (f) Shultz, D. A.; Fico, R. M., Jr.; Bodnar, S. H.; Kumar, K.; Vostrikova, K. E.; Kampf, J. W.; Boyle, P. D. *J. Am. Chem. Soc.* **2003**, *125*, 11761.
 - (14) (a) Michon, P.; Rassat, A. *J. Am. Chem. Soc.* **1975**, *97*, 696. (b) Metzner, E. K.; Libertini, L. J.; Calvin, M. *J. Am. Chem. Soc.* **1977**, *99*, 4500. (c) Berson, J. A. *Acc. Chem. Res.* **1997**, *30*, 238. (d) Frank, N. L.; Cleirac, R.; Sutter, J.-P.; Daro, N.; Kahn, O.; Coulon, C.; Green, M. T.; Golhen, S.; Ouahab, L. *J. Am. Chem. Soc.* **2000**, *122*, 2053.
 - (15) (a) Sato, H.; Kathirvelu, V.; Spagnol, G.; Rajca, S.; Rajca, A.; Eaton, S. S.; Eaton, G. R. *J. Phys. Chem. B* **2008**, *112*, 2818. (b) Rajca, A.; Mukherjee, S.; Pink, M.; Rajca, S. *J. Am. Chem. Soc.* **2006**, *128*, 13497.
 - (16) Zeika, O.; Li, Y.; Jockusch, S.; Parkin, G.; Sattler, A.; Sattler, W.; Turro, N. J. *Org. Lett.* **2010**, *12*, 3696.
 - (17) Frisch, M. J.; Trucks, G. W.; Schlegel, H. B.; Scuseria, G. E.; Robb, M. A.; Cheeseman, J. R.; Scalmani, G.; Barone, V.; Mennucci, B.; Petersson, G. A.; Nakatsuji, H.; Caricato, M.; Li, X.; Hratchian, H. P.; Izmaylov, A. F.; Bloino, J.; Zheng, G.; Sonnenberg, J. L.; Hada, M.; Ehara, M.; Toyota, K.; Fukuda, R.; Hasegawa, J.; Ishida, M.; Nakajima, T.; Honda, Y.; Kitao, O.; Nakai, H.; Vreven, T.; Montgomery, J. A., Jr.; Peralta, J. E.; Ogliaro, F.; Bearpark, M.; Heyd, J. J.; Brothers, E.; Kudin, K. N.; Staroverov, V. N.; Kobayashi, R.; Normand, J.; Raghavachari, K.; Rendell, A.; Burant, J. C.; Iyengar, S. S.; Tomasi, J.; Cossi, M.; Rega, N.; Millam, J. M.; Klene, M.; Knox, J. E.; Cross, J. B.; Bakken, V.; Adamo, C.; Jaramillo, J.; Gomperts, R.; Stratmann, R. E.; Yazyev, O.; Austin, A. J.; Cammi, R.; Pomelli, C.; Ochterski, J. W.; Martin, R. L.; Morokuma, K.; Zakrzewski, V. G.; Voth, G. A.; Salvador, P.; Dannenberg, J. J.; Dapprich, S.; Daniels, A. D.; Farkas, O.; Foresman, J. B.; Ortiz, J. V.; Cioslowski, J.; Fox, D. J.; Gaussian 09, Revision A02; Gaussian Inc.: Wallingford, CT, 2009.
 - (18) Becke, A. D. *J. Chem. Phys.* **1993**, *98*, 5648.
 - (19) Lee, C.; Yang, W.; Parr, R. G. *Phys. Rev. B* **1988**, *37*, 785.
 - (20) Ottaviani, M. F.; Martini, G.; Nuti, L. *Magn. Reson. Chem.* **1987**, *25*, 897.
 - (21) Budil, D. E.; Lee, S.; Saxena, S.; Freed, J. H. *J. Magn. Res. A* **1996**, *120*, 155.
 - (22) Porel, M.; Ottaviani, M. F.; Jockusch, S.; Jayaraj, N.; Turro, N. J.; Ramamurthy, V. *Chem. Commun.* **2010**, *46*, 7736.
 - (23) <http://www.syrres.com/what-we-do/product.aspx?id=854>.
 - (24) Szydłowska, J.; Pietrasik, K.; Głaż, L.; Kaim, A. *Chem. Phys. Lett.* **2008**, *460*, 245.